Precision Calculations in the MSSM

Wolfgang Hollik

Max-Planck-Institut für Physik (Werner-Heisenberg-Institut)
Föhringer Ring 6, D-80805 Munich, Germany
hollik@mppmu.mpg.de

1 Introduction

High-precision experiments at electron-positron and hadron colliders together with the highly accurate measurements of the muon lifetime and gyromagnetic factor impose stringent tests on the standard model and possible extensions. The experimental accuracy in the electroweak observables has reached the level of the quantum effects, and requires the highest standards on the theoretical side as well. A sizeable amount of work has continuously contributed over the last two decades to a steadily rising improvement of the standard model predictions, pinning down the theoretical uncertainties to the level required for the proper interpretation of the precision data. Also for the minimal supersymmetric standard model (MSSM), remarkable progress has to be reported in predicting the precision observables with similar accuracy as in the standard model. Table 1 summarizes the present experimental precision for those high-energy parameters where essential improvements are expected from future collider experiments at the Tevatron (Run II), the LHC, and a e^+e^- Linear Collider with an additional high-luminosity GigaZ option. Moreover, the Z-boson mass and the Fermi constant with their tiny uncertainties [1], $\delta M_Z = 2.1$ MeV and $\delta G_F/G_F = 1 \cdot 10^{-5}$, will also be at our disposal. The availability of both highly accurate measurements and theoretical predictions, at the level of 0.1% precision and better, provides unique tests of the quantum structure of the models and yields indirect informations on yet unexplored heavy sectors.

2 Electroweak precision observables

The possibility of performing precision tests is based on the formulation of the standard model and the MSSM as renormalizable quantum field theories preserving their predictive power beyond tree-level calculations.

Table 1. Present experimental accuracies and expectations for future colliders (see ref. [2] and references therein).

Error for	now	Tev/LHC	LC	GigaZ
M_W [MeV]	33	15	15	6 – 7
$\sin^2\theta_{\rm eff}$	0.00017	0.00021		0.000013
$m_{\rm top}$ [GeV]	5.1	2	0.2	0.13
$M_{\rm Higgs}$ [GeV]	–	0.1	0.05	0.05

2.1 Muon decay and the vector-boson mass correlation

The basic physical quantity for the M_W–M_Z correlation is the muon lifetime τ_μ, which defines the Fermi constant G_F according to

$$\frac{1}{\tau_\mu} = \frac{G_F^2\, m_\mu^5}{192\pi^3}\, F\left(\frac{m_e^2}{m_\mu^2}\right)\left(1+\frac{3}{5}\frac{m_\mu^2}{M_W^2}\right)(1+\Delta_{\rm QED})\,, \tag{1}$$

with $F(x) = 1-8x-12x^2\ln x+8x^3-x^4$. By convention, the QED corrections within the Fermi Model, $\Delta_{\rm QED}$, are included in this defining equation for G_F. The one-loop result for $\Delta_{\rm QED}$ [3] has already been known for several decades; it has recently been supplemented by the two-loop correction [4], yielding

$$\Delta_{\rm QED} = 1 - 1.81\,\frac{\alpha(m_\mu)}{\pi} + 6.7\left(\frac{\alpha(m_\mu)}{\pi}\right)^2, \quad \text{with} \quad \alpha(m_\mu) \simeq \frac{1}{135.90}\,. \tag{2}$$

The tree-level W-propagator effect giving rise to the (numerically insignificant) term $3m_\mu^2/(5M_W^2)$ in (1), is conventionally also included in the definition of G_F, although not part of the Fermi Model prediction. From the precisely measured muon-decay width the value [1] $G_F = (1.16637 \pm 0.00001)\,10^{-5}$ GeV^{-2} for the Fermi constant is derived.

Calculating the muon lifetime within the standard model or the MSSM and comparing the result with (1) yields the relation

$$M_W^2\left(1-\frac{M_W^2}{M_Z^2}\right) = \frac{\pi\alpha}{\sqrt{2}G_F}\,(1+\Delta r)\,, \tag{3}$$

where the radiative corrections are summarized in the quantity Δr. Thereby, a set of infrared-divergent QED-correction graphs has to be removed, which reproduce the QED-correction factor of the Fermi-model result in (1). They have no influence on the relation between G_F and the model parameters.

In the standard model the quantum correction Δr has received a lot of attention. The one-loop result [5] has been improved over the last two decades by numerically important QCD and electroweak higher-order terms, establishing thus a powerful relation that can be used to predict M_W within the SM (or possible extensions), to be confronted with the experimental result for M_W. The quantity Δr depends on the entire set of input parameters. It contains, among others, the on-shell mass counterterms and the photon vacuum polarization from charge renormalization in the classical limit.

The photon vacuum polarization is a basic entry in the predictions for electroweak precision observables. The difference

$$\mathrm{Re}\,\hat{\Pi}^{\gamma}(M_Z^2) = \mathrm{Re}\,\Pi^{\gamma}(M_Z^2) - \Pi^{\gamma}(0) \tag{4}$$

is a finite quantity. The purely fermionic part corresponds to standard QED and does not depend on the details of the electroweak theory. It can be split into a leptonic and a hadronic contribution, yielding the quantity

$$\Delta\alpha = \Delta\alpha_{\mathrm{lept}} + \Delta\alpha_{\mathrm{had}} = -\,\mathrm{Re}\,\hat{\Pi}^{\gamma}_{\mathrm{lept}}(M_Z^2) - \mathrm{Re}\,\hat{\Pi}^{\gamma}_{\mathrm{had}}(M_Z^2)\,, \tag{5}$$

which represents a QED-induced shift in the electromagnetic fine structure constant

$$\alpha \to \alpha(1+\Delta\alpha)\,. \tag{6}$$

It can be resummed [6] according to the renormalization group, accommodating all the leading logarithms of the type $\alpha^n \log^n(M_Z/m_f)$, to give an effective fine-structure constant at the Z mass scale,

$$\alpha(M_Z^2) = \frac{\alpha}{1-\Delta\alpha}\,. \tag{7}$$

The leptonic content of $\Delta\alpha$ can be directly evaluated in terms of the known lepton masses, yielding at three-loop order [7]

$$\Delta\alpha_{\mathrm{lept}} = 314.97687 \cdot 10^{-4}\,. \tag{8}$$

For the light hadronic part, perturbative QCD is not applicable and quark masses are no reasonable input parameters. Instead, the 5-flavour contribution to $\hat{\Pi}^{\gamma}_{\mathrm{had}}$ can be derived from experimental data with the help of a dispersion relation

$$\Delta\alpha_{\mathrm{had}} = -\frac{\alpha}{3\pi}\, M_Z^2\, \mathrm{Re} \int_{4m_\pi^2}^{\infty} \mathrm{d}s'\, \frac{R^{\gamma}(s')}{s'(s'-M_Z^2-i\varepsilon)} \tag{9}$$

where

$$R^{\gamma}(s) = \frac{\sigma(e^+e^- \to \gamma^* \to \mathrm{hadrons})}{\sigma(e^+e^- \to \gamma^* \to \mu^+\mu^-)}$$

is an experimental input quantity for the low energy range. Recent updates including new data points from BES [8] and CMD [9] yield the value $\Delta\alpha = 0.02769 \pm 0.00035$ [10], respectively $\Delta\alpha = 0.02755 \pm 0.00023$ [11].
The heavy quark doublet (t,b) contributes predominantly via the ρ parameter [12],

$$\Delta\rho = \frac{3G_F m_t^2}{8\pi^2\sqrt{2}} \tag{10}$$

to Δr, which thus has a simple form in the light- and heavy-fermion terms at one-loop,

$$\Delta r = \Delta\alpha - \frac{c_W^2}{s_W^2}\,\Delta\rho + \Delta r_{\rm rem}\,. \tag{11}$$

$\Delta\alpha$ contains the large logarithmic corrections from the light fermions and $\Delta\rho$ the quadratic correction from m_t. All other terms are collected in the remainder $\Delta r_{\rm rem}$, which has a typical size of the order ~ 0.01.

Beyond the one-loop order, higher-order 1-particle reducible and irreducible 2- and 3-loop contributions to the ρ parameter have been obtained with electroweak and QCD terms [13]. QCD corrections to Δr beyond the contribution via $\Delta\rho$ are known at $\mathcal{O}(\alpha\alpha_s)$ [14] and $\mathcal{O}(\alpha\alpha_s^2)$ [15]. First approximative electroweak two-loop calculations were performed based on expansions for asymptotically large values of M_H [16] and m_t [17].

In the meantime, the complete electroweak two-loop result in the standard model has become available: the fermionic two-loop terms [18] with all two-loop diagrams for the muon-decay amplitude containing at least one closed fermion loop, and the residual class of the two-loop purely bosonic diagrams [19, 20]. Their influence is displayed in Fig. 1 for the fermionic and in Fig. 2 for the bosonic contributions, in terms of Δr and M_W.

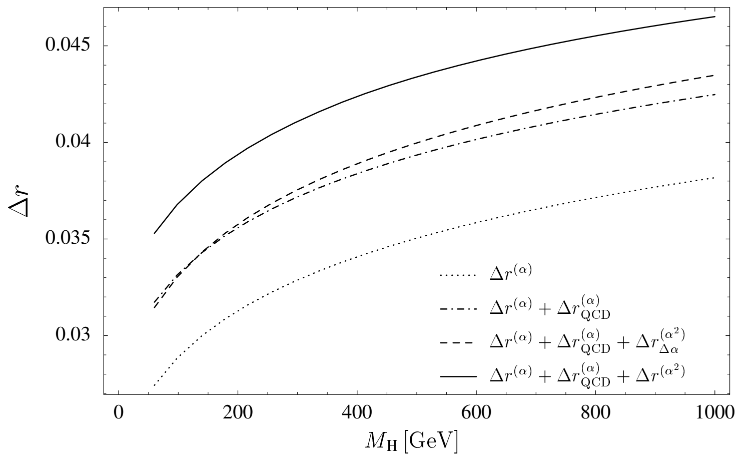

Fig. 1. Various stages of Δr, as a function of M_H. The one-loop contribution, $\Delta r^{(\alpha)}$, is supplemented by the two-loop and three-loop QCD corrections, $\Delta r^{(\alpha)}_{\rm QCD} \equiv \Delta r^{(\alpha\alpha_s)} + \Delta r^{(\alpha\alpha_s^2)}$, and the fermionic electroweak two-loop contributions, $\Delta r^{(\alpha^2)} \equiv \Delta r^{(N_{\rm f}\alpha^2)} + \Delta r^{(N_{\rm f}^2\alpha^2)}$. For comparison, the effect of the two-loop corrections induced by a resummation of $\Delta\alpha$, $\Delta r^{(\alpha^2)}_{\Delta\alpha}$, is shown separately.

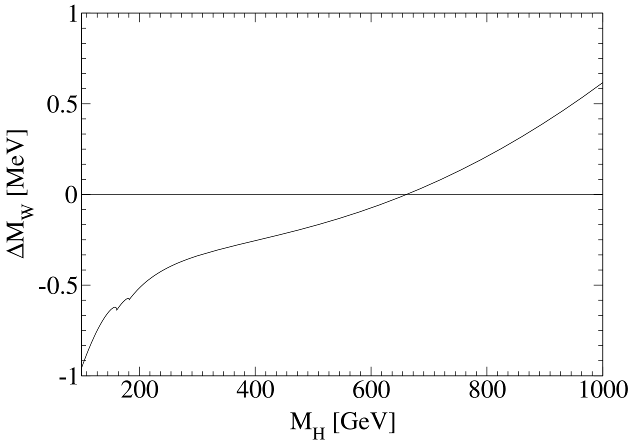

Fig. 2. The shift in M_W from the two-loop bosonic contributions to Δr (from [19]).

2.2 Z boson observables

With M_Z used as a precise input parameter, together with α and G_F, the predictions for the width, partial widths and asymmetries can conveniently be calculated in terms of effective neutral current coupling constants for the various fermions (see e.g. [21]):

$$\begin{aligned} J_\nu^{\rm NC} &= \left(\sqrt{2} G_F M_Z^2\right)^{1/2} (g_V^f \gamma_\nu - g_A^f \gamma_\nu \gamma_5) \\ &= \left(\sqrt{2} G_F M_Z^2 \rho_f\right)^{1/2} \left((I_3^f - 2 Q_f s_f^2)\gamma_\nu - I_3^f \gamma_\nu \gamma_5\right) . \end{aligned} \tag{12}$$

The subleading 2-loop corrections $\sim G_F^2 m_t^2 M_Z^2$ for the leptonic mixing angle [22] s_ℓ^2 have also been obtained in the meantime, as well as for ρ_ℓ [23].

The effective mixing angles are of particular interest, since they determine the on-resonance asymmetries via the combinations

$$A_f = \frac{2 g_V^f g_A^f}{(g_V^f)^2 + (g_A^f)^2} , \tag{13}$$

namely

$$A_{\rm FB} = \frac{3}{4} A_e A_f, \quad A_\tau^{\rm pol} = A_\tau, \quad A_{\rm LR} = A_e . \tag{14}$$

Measurements of the asymmetries hence are measurements of the ratios

$$g_V^f / g_A^f = 1 - 2 Q_f s_f^2 \tag{15}$$

or the effective mixing angles, respectively.

3 Standard model and precision data

3.1 Global fit and Higgs-boson mass

The Z-boson observables form LEP 1 and SLC together with M_W and the top-quark mass from LEP 2 and the Tevatron, constitute the set of high-energy quantities entering a global precision analysis (see [24] for a recent review). From low-energy experiments, the quantity $s_W^2 = M_W/M_Z$ can indirectly be measured in deep-inelastic neutrino–nucleon scattering. The result of the NuTeV collaboration [25] can be expressed as follows,

$$\begin{aligned} s_W^2 &= 0.2277 \pm 0.0013 \pm 0.0009 \\ &\quad -0.00022 \frac{m_t^2 - (175 \text{ GeV})^2}{(50 \text{ GeV})^2} \\ &\quad +0.00032 \ln(M_H/150 \text{ GeV}) \,. \end{aligned}$$

Global fits within the standard model to the electroweak precision data contain M_H as the only free parameter, yielding an upper limit to the Higgs mass at the 95% C.L. of $M_H < 219$ GeV [24], including the present theoretical uncertainties of the standard model predictions. Figure 3, showing the deviation of the individual quantities from the standard model best-fit values, points out the forward-backward asymmetry for b quarks and s_W^2 from deep-inelastic neutrino scattering as the largest deviations from the standard model value for the best fit.

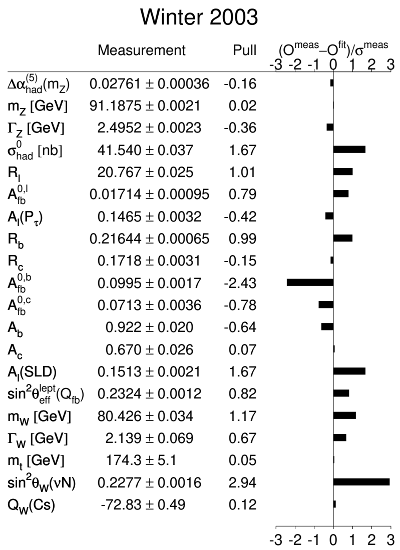

Fig. 3. Experimental results and pulls from a standard model fit [24]. Pull = obs(exp)-obs(SM)/(exp.error).

3.2 Muon anomalous magnetic moment

The anomalous magnetic moment of the muon,

$$a_\mu = \frac{g_\mu - 2}{2} \tag{16}$$

provides a precision test at low energies. The new experimental result of E 821 at Brookhaven National Laboratory [26] has reached a substantial improvement in accuracy. It shows a deviation from the standard model prediction by 2.7 [1.4] standard deviations depending on the evaluation of the hadronic vacuum polarization from data based on e^+e^- annihilation [hadronic τ decays together with isospin rotation], as discussed in [27]. Other recent analyses were performed in [10, 11, 35].

4 The MSSM and precision data

Among the extensions of the standard model, the minimal supersymmetric standard model (MSSM) is the theoretically favoured scenario as the most predictive framework beyond the standard model. A definite prediction of the MSSM is the existence of a light Higgs boson with mass below $\sim$ 135 GeV [28]. The detection of a light Higgs boson could be a significant hint for supersymmetry.

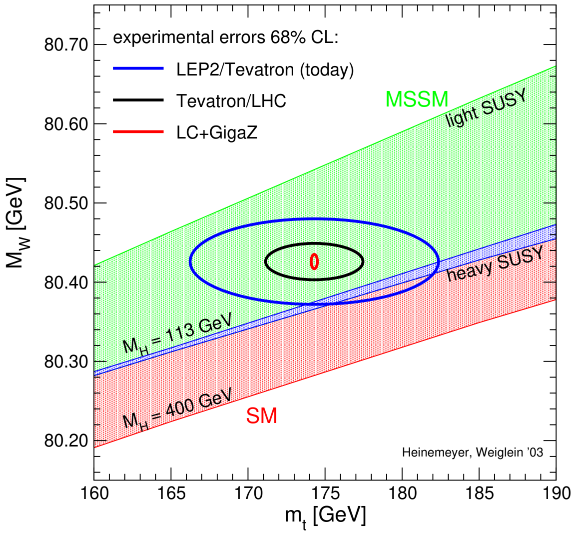

Fig. 4. The W mass range in the standard model (lower band) and in the MSSM (upper band). Bounds are from the non-observation of Higgs bosons and SUSY particles.

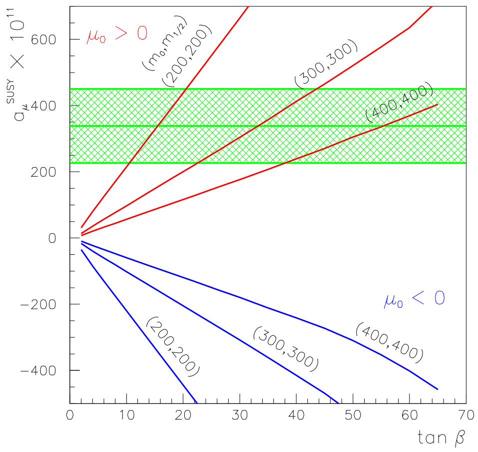

Fig. 5. Supersymmetric contribution to a_μ [37]. The deviation of the measured value from the standard model prediction is indicated by the horizontal band.

The structure of the MSSM as a renormalizable quantum field theory allows a similarly complete calculation of the electroweak precision observables as in the standard model in terms of one Higgs mass (usually taken as the CP-odd 'pseudoscalar' mass M_A) and $\tan\beta = v_2/v_1$, together with the set of SUSY soft-breaking parameters fixing the chargino/neutralino and scalar fermion sectors. The general discussion of renormalization of the MSSM to all orders with implications on the structure of the counter terms is given in [29]. Complete 1-loop calculations are available for Δr [30] and for the Z boson observables [31].

A possible mass splitting between $\tilde{b}_L$ and $\tilde{t}_L$ yields a contribution to the ρ-parameter of the same sign as the standard top term. As a universal loop contribution, it enters the quantity Δr and the Z boson couplings and is thus significantly constrained by the data The 2-loop α_s-corrections have been computed in [32], and the electroweak 2-loop contribution from the Yukawa couplings in [33].

As an example, Figure 4 displays the range of predictions for M_W in the minimal model and in the MSSM, together with the present experimental errors and the expectations for the future collliders LHC and LC. As can be seen, the MSSM prediction is in better agreement with the present data, although not conclusive as yet. Future increase in the experimental accuracy, however, will become decisive for the separation between the models.

Especially for the muonic $g-2$, the MSSM can significantly improve the agreement between theory and experiment: relatively light scalar muons, muon-sneutrinos and charginos/neutralinos, together with a large value of

$\tan\beta$ can provide a positive contribution Δa_μ which can entirely explain the difference $a_\mu^{\rm exp} - a_\mu^{\rm SM}$ [34]. Figure 5 illustrates the MSSM contribution for universal SUSY scalar mass parameters m_0 and spin-1/2 mass parameters $m_{1/2}$.

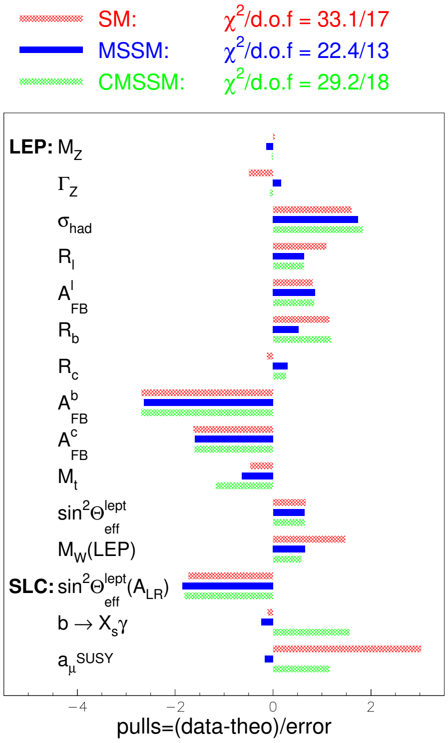

Fig. 6. Best fits in the SM and in the MSSM, normalized to the data [37]. Error bars are those from data.

The MSSM yields a comprehensive description of the precision data, in a similar way as the standard model does. Global fits, varying the MSSM parameters, are available [36] to all electroweak precision data. They have been updated [37], showing that the description within the MSSM is slightly better than in the standard model. This is mainly due to the improved agreement for a_μ (see Figure 6). The situation for $A_{\rm FB}^{\rm b}$, however, remains unaltered.

As far as the deviation of the NuTeV result (16) from the standard model prediction is concerned, the MSSM fails to improve the situation [38].

5 The light Higgs boson of the MSSM

The existence of a light Higgs boson, in the mass range below 135 GeV, is a definite prediction of the MSSM. In contrast to the standard model, its mass m_h is not a free parameter but depends on the other parameters of the model. The prediction for m_h, therefore, is a crucial theoretical tool to probe the MSSM parameter space. From the experimental side, the Higgs mass can be measured with high accuracy [2]: 100 MeV at the LHC, and 50 MeV at a Linear e^+e^- Collider. m_h is, hence, another precision observable in the MSSM. The precise theoretical value is very sensitive to higher-order effects (see [28] for recent results and references given therein). An illustrative example is shown in Figure 7.

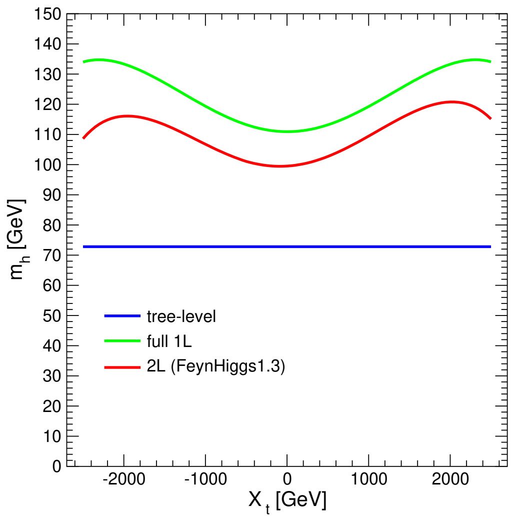

Fig. 7. The lightest Higgs-boson mass in the MSSM, in various orders of perturbation theory [39]. SUSY parameters: $\tan\beta = 3$, $M_{\tilde{Q}} = M_2 = \mu = M_A = 1$ TeV, $m_{\tilde{g}} = 800$ GeV. X_t is the non-diagonal entry in the top-squark mass matrix.

6 SUSY particles

Experiments at future high-energy colliders will be able to discover supersymmetric particles and to investigate their properties. Provided their masses are not too high, a linear electron-positron collider will be the best environment for precision studies of supersymmetric models [40], especially of the MSSM. From precise measurements of masses, cross sections and asymmetries in chargino and neutralino production, the fundamental parameters can be reconstructed [41], to shed light on the mechanism of SUSY breaking.

In view of the experimental prospects it is inevitable to include higher-order terms in the calculation of the measureable quantities in order to achieve theoretical predictions matching the experimental accuracy. Studies on chargino-pair production [42, 43, 44], neutralino-pair production [45], scalar-quark decays [46], and sfermion-pair production [47] have demonstrated that Born-level predictions can be influenced significantly by one-loop radiative corrections. In [44, 46], with complete one-loop calculations performed in on-shell renormalization schemes, it was shown explicitly that besides the fermion- and sfermion-loop contributions also the virtual contributions from the supersymmetric gauge and Higgs sector are not negligible.

Since the masses of charginos and neutralinos are among the precision observables with lots of information on the SUSY-breaking structure, the relations between the particle masses and the SUSY parameters as well as the relations between the masses themselves are important theoretical objects for precision calculations. Previous studies were done in the $\overline{\mathrm{MS}}$ renormalization scheme [48, 49] with running parameters. In [50, 51] on-shell scheme calculations were performed yielding the one-loop corrected mass eigenvalues. In a similar way, the sfermion-mass spectrum, including complete one-loop contributions, was obtained [52].

On-shell renormalization is specified in particular by treating all particle masses as pole masses, and, optionally, with field renormalization implemented in a way that allows to formulate the renormalized 2-point vertex functions as UV-finite matrices which become diagonal for external momenta on-shell. The masses of the two charginos and of one neutralino are used as input to fix the MSSM parameters μ, M_1, M_2. Since only the gaugino-mass parameters M_1, M_2 and the Higgsino-mass parameter μ can be renormalized independently in terms of three pole masses, with all other renormalization constants fixed in the gauge and Higgs sector, the residual eigenvalues of the tree-level mass matrices are no longer the pole positions of the corresponding dressed propagators; the pole masses hence receive a shift versus the tree-level masses, which is calculable in terms of the renormalized self-energies. At one-loop order, the following relation

$$m_{\tilde{\chi}^0_i} = m_i \left[1 - \mathrm{Re}\, \hat{\Sigma}^L_{ii}(m_i^2)\right] - \mathrm{Re}\, \hat{\Sigma}^{SL}_{ii}(m_i^2) \tag{17}$$

holds for the neutralino pole masses with $i = 2, 3, 4$, with respect to their tree-level masses m_i. The renormalized self-energies in the Lorentz-decomposition, with the left/right projectors $\omega_{L/R}$,

$$\hat{\Sigma}_{ij}(p) = \not{p}\, \omega_L \hat{\Sigma}^L_{ij}(p^2) + \not{p}\, \omega_R \hat{\Sigma}^R_{ij}(p^2) + \omega_L \hat{\Sigma}^{SL}_{ij}(p^2) + \omega_R \hat{\Sigma}^{SR}_{ij}(p^2)\,,$$

provide the scalar self-energy functions in (17).

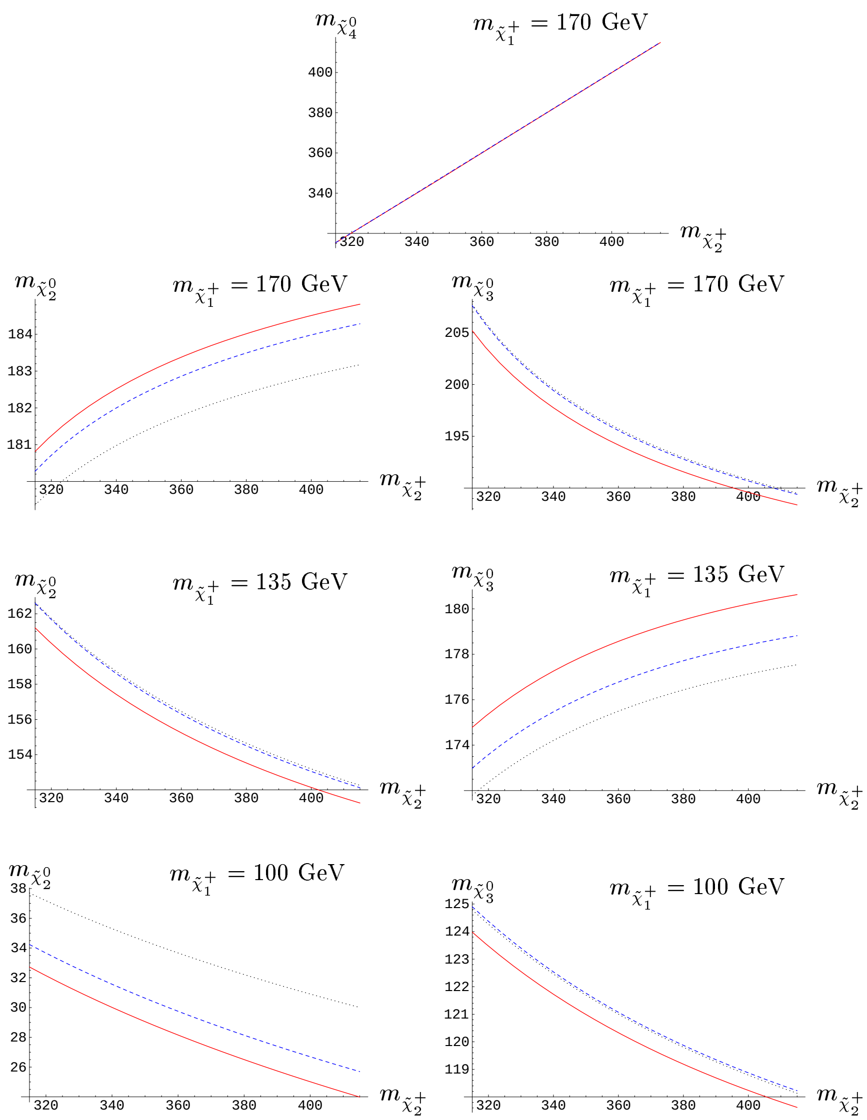

Fig. 8. Dependence of the derived neutralino masses (in GeV) on the chargino masses $m_{\tilde{\chi}_1^+}$ and $m_{\tilde{\chi}_2^+}$. Born approximation (dotted, black), including loop corrections with (s)fermions only (dashed, blue), and with the complete one-loop contributions (solid, red). The input neutralino mass is chosen as $m_{\tilde{\chi}_1^0} = 110$ GeV throughout all diagrams. The plots for $m_{\tilde{\chi}_4^0}$ are practically indistinguishable for all three different values of $m_{\tilde{\chi}_1^+}$.

As an example, Fig. 8 shows the dependence of the neutralino masses on the input mass $m_{\tilde{\chi}_2^+}$ of the heavy chargino at three different values for the mass $m_{\tilde{\chi}_1^+}$ of the light chargino. Depicted are: the tree-level approximation of the calculated neutralino masses, their values after including the corrections from the (s)fermionic loops only, and finally the complete one-loop corrected masses with all MSSM particles in the virtual states. For the heaviest neutralino mass $m_{\tilde{\chi}_4^0}$ the shift is small, not more than 175 MeV throughout the whole scanned parameter space, and nearly invisible in the graphical illustration. Accordingly, the relative corrections are less than 0.05 % everywhere, and hence we do not give more than one graph in the figure. More details can be found in [50].

7 Conclusions

The experimental data for tests of the standard model have achieved an impressive accuracy. In the meantime, many theoretical contributions have become available to improve and stabilize the standard model predictions and to reach a theoretical accuracy clearly better than 0.1%.

The MSSM, mainly theoretically advocated, is competitive to the standard model in describing the data with improvements in specific observables, although not conclusive. Since the MSSM predicts the existence of a light Higgs boson, the detection of a Higgs particle could be an indication of supersymmetry. It is therefore highly important to study the different features of such a Higgs boson in the various models at a level of high precision. Moreover, precision studies of supersymmetric particles will become necessary for revealing the mechanism of SUSY breaking and will require a proper inclusion of higher-order effects as well.

References

1. Particle Data Group, K. Hagiwara et al., *Phys. Rev.* D **66**, 010001 (2002)
2. J. Erler, S. Heinemeyer, W. Hollik, G. Weiglein, P.M. Zerwas, *Phys. Lett.* B **486**, 125 (2000); U. Baur et al., hep-ph/0111314
3. R.E. Behrends, R.J. Finkelstein, A. Sirlin, Phys. Rev **101**, 866 (1956); S.M. Berman, Phys. Rev. **112**, 267 (1958); T. Kinoshita, A. Sirlin, Phys. Rev. **113**, 1652 (1959)
4. T. van Ritbergen, R.G. Stuart, *Phys. Rev. Lett.* **82**, 488 (1999); *Phys. Lett.* B **564**, 343 (2000);
   M. Steinhauser, T. Seidensticker, *Phys. Lett.* B **467**, 271 (1999)
5. A. Sirlin, *Phys. Rev.* D **22**, 971 (1980); W.J. Marciano, A. Sirlin, *Phys. Rev.* D **22**, 2695 (1980)
6. W.J. Marciano, *Phys. Rev.* D **20**, 274 (1979)
7. G. Källén, A. Sabry, *K. Dan. Vidensk. Selsk. Mat.-Fys. Medd.* **29** (1955) No. 17; M. Steinhauser, *Phys. Lett.* B **429**, 158 (1998)

8. BES Collaboration, J.Z. Bai et al., *Phys. Rev. Lett.* **84**, 594 (2000); **88**, 101802 (2002)
9. CMD-2 Collaboration, R.R. Akhmetshin et al., *Phys. Lett.* B **527**, 161 (2002)
10. F. Jegerlehner, *J. Phys.* G **29**, 101 (2003); hep-ph/0312372
11. K. Hagiwara, A.D. Martin, D. Nomura, T. Teubner, hep-ph/0312250
12. D. Ross, M. Veltman, *Nucl. Phys.* B **95**, 135 (1975); M. Veltman, *Nucl. Phys.* B **123**, 89 (1977); M.S. Chanowitz, M.A. Furman, I. Hinchliffe, *Phys. Lett.* B **78**, 285 (1978)
13. M. Consoli, W. Hollik, F. Jegerlehner, *Phys. Lett.* B **227**, 167 (1989); J. van der Bij, F. Hoogeveen, *Nucl. Phys.* B **283**, 477 (1987; R. Barbieri, M. Beccaria, P. Ciafaloni, G. Curci, A. Vicere, *Phys. Lett.* B **288**, 95 (1992); *Nucl. Phys.* B **409**, 105 (1993); J. Fleischer, O.V. Tarasov, F. Jegerlehner, *Phys. Lett.* B **319**, 249 (1993) and *Phys. Rev.* D **51**, 3820 (1995); A. Djouadi, C. Verzegnassi, *Phys. Lett.* B **195**, 265 (1987); L. Avdeev, J. Fleischer, S.M. Mikhailov, O. Tarasov, *Phys. Lett.* B **336**, 560 (1994); E: **349**, 597 (1995); K. Chetyrkin, J. Kühn, M. Steinhauser, *Phys. Lett.* B **351**, 331 (1995); J. van der Bij, K. Chetyrkin, M. Faisst, G. Jikia, T. Seidensticker, *Phys. Lett.* B **498**, 156 (2001); M. Faisst, J. Kühn, T. Seidensticker, O. Veretin, *Nucl. Phys.* B **665**, 649 (2003)
14. B.A. Kniehl, *Nucl. Phys.* B **347**, 89 (1990); F. Halzen, B.A. Kniehl, *Nucl. Phys.* B **353**, 567 (1991); B.A. Kniehl, A. Sirlin, *Nucl. Phys.* B **371**, 141 (1992), *Phys. Rev.* D **47**, 883 (1993); A. Djouadi, P. Gambino, *Phys. Rev.* D **49**, 3499 (1994);
15. K. Chetyrkin, J. Kühn, M. Steinhauser, *Phys. Rev. Lett.* **75**, 3394 (1995)
16. J. van der Bij, M. Veltman, *Nucl. Phys.* B **231**, 205 (1984)
17. G. Degrassi, P. Gambino, A. Vicini, *Phys. Lett.* B **383**, 219 (1996); G. Degrassi, P. Gambino, M. Passera, A. Sirlin, *Phys. Lett.* B **418**, 209 (1998)
18. A. Freitas, W. Hollik, W. Walter, G. Weiglein, *Phys. Lett.* B **495**, 338 (2000); *Nucl. Phys.* B **632**, 189 (2002); M. Awramik, M. Czakon, *Phys. Lett.* B **568**, 48 (2003)
19. M. Awramik, M. Czakon, *Phys. Rev. Lett.* **89**, 241801 (2002)
20. A. Onishchenko, O. Veretin, *Phys. Lett.* B **551**, 111 (2003); M. Awramik, M. Czakon, A. Onishchenko, O. Veretin, *Phys. Rev.* D **68**, 053004 (2003)
21. D. Bardin et al., *Reports of the Working Group on Precision Calculations for the Z Resonance*, p. 7, CERN 95-03 (1995), eds. D. Bardin, W. Hollik, G. Passarino; hep-ph/9709229
22. G. Degrassi, P. Gambino, A. Sirlin, *Phys. Lett.* B **394**, 188 (1997)
23. G. Degrassi, P. Gambino, *Nucl. Phys.* B **567**, 3 (2000)
24. M. Grünewald, hep-ex/0304023; The LEP Collaborations, the LEP Electroweak Working Group, the SLD Electroweak and Heavy Flavour Working Groups, hep-ex/0312023
25. NuTeV Collaboration, G. Zeller et al., *Phys. Rev. Lett.* **88**, 091802
26. H.N. Brown et al., *Phys. Rev. Lett.* **86**, 2227 (2001); G.W. Bennett et al., *Phys. Rev. Lett.* **89**, 101804 (2002) and hep-ex/0401008
27. M. Davier, S. Eidelman, A. Höcker, Z. Zhang, *Eur. Phys. J.* C **27**, 497 (2003); S. Ghozzi, F. Jegerlehner, *Phys. Lett.* B **583**, 222 (2004)
28. G. Degrassi, S. Heinemeyer, W. Hollik, P. Slavich, G. Weiglein, *Eur. Phys. J.* C **28**, 133 (2003)
29. W. Hollik, E. Kraus, M. Roth, C. Rupp, K. Sibold, D. Stöckinger, *Nucl. Phys.* B **639**, 3 (2002)

30. P. Chankowski, A. Dabelstein, W. Hollik, W. Mösle, S. Pokorski, J. Rosiek, *Nucl. Phys.* B **417**, 101 (1994); D. Garcia, J. Solà, *Mod. Phys. Lett.* A **9**, 211 (1994)
31. D. Garcia, R. Jiménez, J. Solà, *Phys. Lett.* B **347**, 309 and 321 (1995); D. Garcia, J. Solà, *Phys. Lett.* B **357**, 349 (1995); A. Dabelstein, W. Hollik, W. Mösle, in *Perspectives for Electroweak Interactions in* e^+e^- *Collisions*, Ringberg Castle 1995, ed. B.A. Kniehl, World Scientific 1995 (p. 345); P. Chankowski, S. Pokorski, *Nucl. Phys.* B **475**, 3 (1996); J. Bagger, K. Matchev, D. Pierce, R. Zhang, *Nucl. Phys.* B **491**, 3 (1997)
32. A. Djouadi, P. Gambino, S. Heinemeyer, W. Hollik, C. Jünger, G. Weiglein, *Phys. Rev. Lett.* **78**, 3626 (1997) and *Phys. Rev.* D **57**, 4179 (1998)
33. S. Heinemeyer, G. Weiglein, *JHEP* **0210**, 072 (2002) and hep-ph/0301062
34. A. Czarnecki, W. Marciano, *Phys. Rev.* D **64**, 013014 (2001)
35. J.F. de Trocóniz, F.J. Ynduráin, hep-ph/0402285
36. W. de Boer, A. Dabelstein, W. Hollik, W. Mösle, U. Schwickerath, *Z. Phys.* C **75**, 627 (1997)
37. W. de Boer, C. Sander, Proceedings of *SUSY 02*, eds. P. Nath and P.M. Zerwas, Hamburg 2002
38. S. Davidson, S. Forte, P. Gambino, N. Rius, A. Strumia, *JHEP* **0202**, 037 (2002); A. Kurylov, M.J. Ramsey-Musolf, S. Su, *Nucl. Phys.* B **667**, 321 (2003)
39. S. Heinemeyer, W. Hollik, G. Weiglein, *Comp. Phys. Comm.* **124**, 76 (2000). The updated version of *FeynHiggs* is available at `http://www.feynhiggs.de`
40. TESLA Technical Design Report, DESY 2001-011, Part III, R. Heuer, D. Miller, F. Richard, P. Zerwas (eds.), hep-ph/0106315
41. S.Y. Choi, A. Djouadi, M. Guchait, J. Kalinowski, H.S. Song, P.M. Zerwas, *Eur. Phys. J.* C **14**, 535 (2000) G. Moortgat-Pick, A. Bartl, H. Fraas, W. Majerotto, hep-ph/0004181; S.Y. Choi, J. Kalinowski, G. Moortgat-Pick, P.M. Zerwas, hep-ph/0108117 and hep-ph/00202139; J. Kalinowski, G. Moortgat-Pick, hep-ph/0202083; hep-ph/0202084
42. M. A. Díaz, S. F. King, D. A. Ross, *Nucl. Phys.* B **529**, 23 (1998)
43. S. Kiyoura, M. M. Nojiri, D. M. Pierce, Y. Yamada, *Phys. Rev.* D **58**, 075002 (1998)
44. T. Blank, W. Hollik, hep-ph/0011092
45. W. Öller, H. Eberl, W. Majerotto, hep-ph/0402134
46. J. Guasch, W. Hollik, J. Solà, *Phys. Lett.* B **510**, 211 (2001) and *JHEP* **10**, 040 (2002)
47. A. Arhrib, W. Hollik, hep-ph/0311149; K. Kovarik, C. Weber, H. Eberl, W. Majerotto, hep-ph/0401092
48. D. Pierce, A. Papadopoulos, *Phys. Rev.* D **50**, 565 (1994) and *Nucl. Phys.* B **430**, 278 (1994)
49. A. B. Lahanas, K. Tamvakis, N. D. Tracas, *Phys. Lett.* B 324, 387 1994
50. T. Fritzsche, W. Hollik, *Eur. Phys. J.* C **24**, 619 (2002)
51. H. Eberl, M. Kincel, W. Majerotto, Y. Yamada, *Phys. Rev.* D **64**, 115013 (2001); W. Öller, H. Eberl, W. Majerotto, C. Weber, *Eur. Phys. J.* C **29**, 563 (2002)
52. W. Hollik, H. Rzehak, *Eur. Phys. J.* C **32**, 127 (2003)